The mitotic-spindle-associated protein astrin is essential for progression through mitosis

Jens Gruber[1,*], Jens Harborth[1,*], Jörg Schnabel[1], Klaus Weber[1] and Mechthild Hatzfeld[2,‡]

[1]Max Planck Institute for Biophysical Chemistry, Department of Biochemistry, Am Fassberg 11 37070 Göttingen, Germany
[2]Department of Biochemistry and Pathobiochemistry, Medical Faculty of the University of Halle, 06097 Halle/Saale, Germany
*These authors contributed equally to this work
‡Author for correspondence (e-mail: mechthild.hatzfeld@medizin.uni-halle.de)

Accepted 3 August 2002
Journal of Cell Science 115, 4053-4059 © 2002 The Company of Biologists Ltd
doi:10.1242/jcs.00088

Summary

Astrin is a mitotic-spindle-associated protein expressed in most human cell lines and tissues. However, its functions in spindle organization and mitosis have not yet been determined. Sequence analysis revealed that astrin has an N-terminal globular domain and an extended coiled-coil domain. Recombinant astrin was purified and characterized by CD spectroscopy and electron microscopy. Astrin showed parallel dimers with head-stalk structures reminiscent of motor proteins, although no sequence similarities to known motor proteins were found. In physiological buffers, astrin dimers oligomerized via their globular head domains and formed aster-like structures. Silencing of astrin in HeLa cells by RNA interference resulted in growth arrest, with formation of multipolar and highly disordered spindles. Chromosomes did not congress to the spindle equator and remained dispersed. Cells depleted of astrin were normal during interphase but were unable to progress through mitosis and finally ended in apoptotic cell death. Possible functions of astrin in mitotic spindle organization are discussed.

Key words: Astrin, Coiled coil, Microtubules, Mitotic spindle, RNA interference

Introduction

The mitotic spindle, a bipolar microtubule-based structure, is responsible for accurate chromosome segregation during mitosis (Compton, 2000). The basic structural element of the spindle is an antiparallel array of microtubules with their minus ends anchored at the spindle poles and their plus ends projecting towards the chromosomes. This polar lattice of microtubules serves as a track for motors of the dynein and kinesin superfamily (Hirokawa et al., 1998a; Kim and Endow, 2000). Spindle microtubules are highly dynamic structures with a half-life of 60-90 seconds, and this dynamic instability is fundamental to mitotic spindle structure and regulation (Joshi, 1998; Saxton et al., 1984). Several tubulin-binding proteins promote microtubule depolymerization, whereas other microtubule-associated proteins (MAPs) counteract the destabilizing effect, and some evidence suggests that cell-cycle-dependent regulation of these two protein families by cyclin-dependent kinase 1 is involved in regulating the fast turnover of mitotic microtubules compared to interphase microtubules (Tournebize et al., 2000; Vasquez et al., 1999; Wittmann et al., 2001). Microtubule motor proteins have an important function in spindle organization. These proteins have been divided into two classes, the kinesin superfamily, which includes both plus- and minus-end-directed motors and the minus-end-directed motor protein dynein. Different kinesins cooperate and counteract during the process of spindle assembly. Oligomeric motor complexes that crosslink and move along microtubules have been shown to be sufficient for self-organization of tubulin asters in vitro (Heald et al., 1996; Karsenti and Vernos, 2001; Nedelec et al., 1997; Walczak et al., 1998; Wittmann et al., 2001).

The primary function of the mitotic spindle is to segregate chromosomes such that a complete set of chromosomes ends up at each spindle pole. The process of segregation depends on a complex interplay between forces generated by motor proteins associated with spindle microtubules, kinetochores and chromosome arms as well as dynamic instability of spindle microtubules (Howell et al., 2001; Maney et al., 2000; Nicklas et al., 1995; Rieder et al., 1995; Rieder and Salmon, 1998). Chromosome separation also depends on attachment of chromosomes to spindle microtubules via their kinetochores, and it has been shown that cytoplasmic dynein as well as several kinesin family members localize at the kinetochore (Banks and Heald, 2001). CENP-E is another kinesin-like protein that is part of a kinetochore-associated signalling pathway that monitors kinetochore-microtubule attachment and ensures high segregation fidelity. Depletion of CENP-E from mammalian kinetochores leads to a reduction of kinetochore-microtubule binding and mitotic arrest, producing a mixture of aligned and unaligned chromosomes (Abrieu et al., 2000; Lombillo et al., 1995; Yao et al., 2000; Yen et al., 1992).

In order to gain more insight into spindle organization, Mack and Compton used mitotic microtubules prepared from Hela cell extracts to identify spindle-associated proteins in an elegant mass spectroscopic analysis (Mack and Compton, 2001). Several proteins with functional roles in spindle assembly and a novel non-motor coiled-coil protein named astrin were described. Using immunofluorescence and ectopic expression of the GFP-tagged astrin, its spindle localization during mitosis was confirmed (Mack and Compton, 2001). We originally identified an astrin cDNA clone in a two-hybrid

screen with a keratin 18 bait although this interaction could not be confirmed using other methods. We named the full-length 3,793 bp cDNA *DEEPEST* because the predicted protein contains this sequence motif. Antibodies located the protein to the spindle, and sequence predictions indicated two long coiled coils. When we entered the cDNA sequence into the EMBL/GenBank databases in May 1998 we added information concerning a coiled-coil protein associated with the mitotic spindle apparatus (accession number AF 063308). Owing to a sequence error at position 3341, our predicted protein sequence lacked the C-terminal 101 amino acids provided by Mack and Compton (accession number AF 399910). The same protein sequence including the sequence error of our original DEEPEST-sequence was also provided by Chang et al. (Chang et al., 2001) (accession number P33176 and NM 006461), who called this protein hMAP126. hMAP126 has been described as a mitotic-spindle-associated protein that is post-translationally modified by cdk1 phosphorylation. To avoid confusion we have dropped the name DEEPEST and use instead the name astrin.

Here, we describe a more detailed characterization of astrin's domain organization and function in spindle pole organization. Astrin has a domain structure resembling that of motor proteins with a large head domain, which lacks sequence similarity to motor domains, and a coiled-coil domain responsible for formation of parallel dimers. Under physiological conditions, recombinant astrin dimers oligomerize via their head domains into aster-like structures. Moreover, we show that astrin is essential for progression through mitosis. Depletion of astrin by RNA interference resulted in the formation of multipolar and highly disordered spindles and lead to growth arrest and apoptotic cell death. These results indicate that astrin has a critical role in assembly or orientation of the bipolar structure of the spindle.

Materials and Methods

cDNA cloning and sequence analysis

RNA from MCF-7 and HeLa cells was prepared using the LiCl/urea extraction method (Auffrey and Rougeon, 1980). PolyA$^+$-RNA was prepared using the Oligotex mRNA kit (Qiagen, Hilden, Germany). Starting from 5 μg of polyA$^+$-RNA, a cDNA library of MCF-7 cells was constructed in the phagemid pAD-GAL4 (GAL4 activation domain vector) using the HybriZAP two-hybrid cDNA Gigapack cloning kit (Stratagene, LaJolla, CA, USA). cDNA synthesis was oligo-dT primed. A two-hybrid screen with a keratin 18 bait revealed a partial astrin cDNA of 1300 bp. Using the digoxigenin-labeled 5′ end as a probe (Roche, Mannheim FRG), two overlapping clones of 887 bp and 1290 bp were obtained. The 5′ end of the cDNA was amplified by 5′-RACE PCR using the 5′/3′-RACE kit (Roche) with the following primers: (1) TGC CAT GGT ATC TAA ACG GGC; (2) CAG ATC GTC TGT TCT CAA AGG; and (3) TGC CAT GGT ATC TAA ACG GGC. Automated sequencing of both strands was performed (kit and sequencer model 373a, Applied Biosystems, Foster City, CA, USA).

Astrin cDNA expression constructs were generated by rt-PCR with total RNA from MCF-7 cells. Suitable restriction sites were included in the primer sequences. The following constructs were used in this study: (1) Astrin DN: aa 1-356. Fragment DN was cloned into *Bam*HI/*Hin*dIII sites of pET-23a. (2) Astrin DC: aa 707-1027. Fragment DC was cloned into pGEX-2T (Pharmacia Biotech). This vector contains an N-terminal glutathione-S-transferase (GST)-tag sequence. (3) Astrin 1-1,123 was cloned into pET23a for prokaryotic expression (astrin-T7). This construct lacks the C-terminal 70 amino acids of full-length astrin. Fig. 1B gives an overview of constructs used in this study.

Expression and purification of recombinant polypeptides

Constructs in pET-23a (astrin-T7, aa 1-1,123 and DN aa 1-356) were expressed in *Escherichia coli* BL21 (DE3) pLysS. GST-DC (aa 707-1027) was expressed in *E. coli* strain Xl1 blue.

Astrin-DN was soluble and purified from bacteria by anion exchange chromatography on a MonoQ column and gel filtration on Sephadex 75. Astrin-T7 aggregated into inclusion bodies, which were prepared according to Hatzfeld and Weber and solubilized in urea buffer (8.5 M urea, 10 mM Tris-HCl pH 8, 5 mM EDTA, 2.5 mM DTT) (Hatzfeld and Weber, 1990). Astrin-T7 was purified to homogeneity from this solution by anion exchange chromatography on MonoQ column. The GST-DC fusion protein was soluble and purified on glutathione sepharose matrix (Pharmacia Biotech) in PBS (8 mM Na_2HPO_4, 1.5 mM KH_2PO_4, 140 mM NaCl, 3.7 mM KCl). The GST-tag was cleaved by thrombin digestion, and astrin was eluted in PBS.

CD spectroscopy

Purified recombinant astrin-T7 protein at a concentration of about 0.2 mg/ml was dialyzed against 8 mM Na_2HPO_4, 1.5 mM KH_2PO_4, 0.5 mM DTT (pH 7.5) at 4°C overnight. The extinction at 280 nm was measured. Protein concentration was determined using the corresponding extinction coefficient calculated from the deduced amino-acid sequence of the construct. CD spectra from 200 to 250

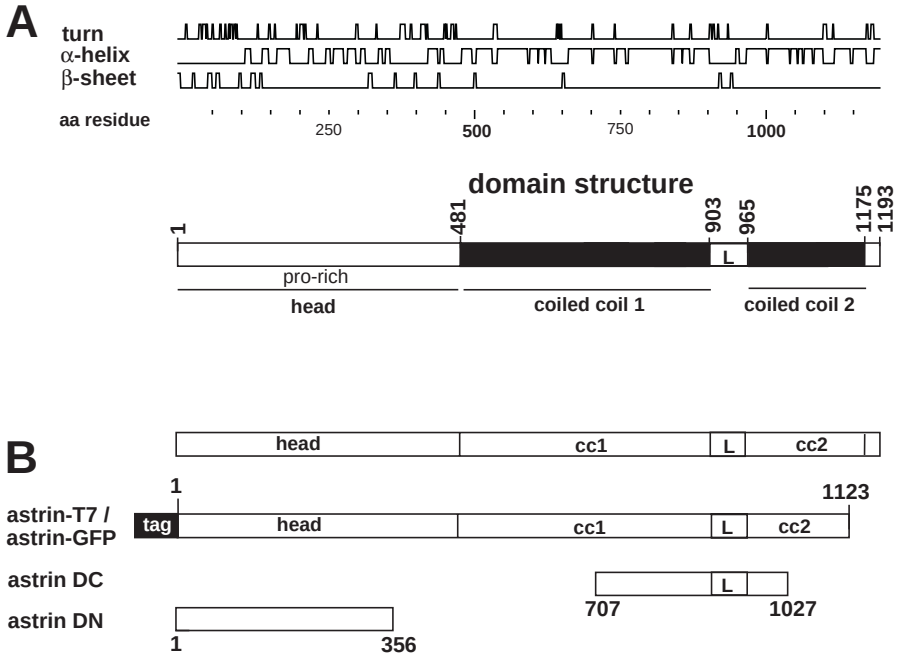

Fig. 1. (A) Secondary structure prediction and domain organization of astrin. (B) cDNA constructs used in this study. cc denotes the coiled-coil regions, L the linker region.

nm (stepsize 0.5 nm, speed 50 nm/minute) were measured with the polarimeter J-720 (Jasco, Groß-Umstadt, Germany) in a cuvette of 0.1 cm thickness. For comparison, α-tropomyosin from bovine brain (which has an α-helix content greater than 90%; the protein was kindly provided by N. Geisler) was measured in the same buffer. CD spectra of poly-L-lysine were measured under the following conditions: 0.1 N KOH (100% α-helix), 0.1 N KOH after incubation at 60°C for 2 hours (100% β-strand) and 0.1 N HCl (100% random coil). The relative α-helix content of recombinant astrin-T7 was determined by comparing its molecular ellipticity at the isosbestic point of poly-L-lysine β-strand/random coil (208 nm) with the molecular ellipticity of 100% α-helical poly-L-lysine at the same wavelength.

Electron microscopy

Recombinant astrin-T7 protein was microdialyzed for 3 hours at room temperature either against PBS containing 2.5 mM DTT or phosphate buffer without salt (8 mM Na_2HPO_4, 1.5 mM KH_2PO_4, 2.5 mM DTT). After dialysis, glycerol was added to 33% of the volume, samples were sprayed onto mica sheets, rotary shadowed at an angle of 4° first with platinum/carbon at 700 Hz and then with carbon at 60 Hz in a vacuum rotary shadowing device (Baltzers, Liechtenstein) and inspected with a CM-12 transmission electron microscope (Phillips, Eindhoven, The Netherlands).

Antibody to astrin

Recombinant astrin fragments covering amino-acid residues 1-363 (astrin-DN) and 707-1027 (astrin-DC) were purified from *E. coli* and used to elicit rabbit antibodies. An aliquot of the truncated astrin was coupled to Sepharose 4B and used to obtain antigen affinity-purified rabbit antibodies. Purified astrin antibodies eluted with low pH buffer were immediately neutralized with Tris-base.

Gel electrophoresis and western blot analysis

SDS gel electrophoresis and western blotting were performed according to standard protocols.

A monoclonal antibody against the T7-tag was obtained from Novagen (Calbiochem-Novabiochem, Schwalbach FRG), and affinity-purified horseradish-conjugated rabbit anti-mouse and swine anti-rabbit immunoglobulins were from Dako, (Copenhagen, Denmark). Bands were detected using ECL (Amersham Pharmacia).

Silencing of astrin by siRNA

RNA interference mediated by duplexes of 21-nt RNAs was performed on human HeLa cells as described previously (Elbashir et al., 2001; Harborth et al., 2001). The siRNA sequence for targeting astrin was from position 2639 to 2661, relative to the first nucleotide of the start codon (GenBank accession number AF 399910). As an siRNA control, a sequence targeting firefly (*Photinus pyralis*) luciferase (accession number X 65324) at positions 153 to 175 was used (pGL2 siRNA). The 21-nt RNAs were chemically synthesized by Dharmacon (Lafayette, CO, USA) and delivered in a salt-free and deprotected form. Duplexes were formed as before. Alternatively, duplexes were obtained commercially. Transfection with Oligofectamine (Invitrogen; lot number 1122079) was as described previously (Harborth et al., 2001). Cells were monitored by phase microscopy at intervals, and after 44 hours, they were analyzed by immunofluorescence microscopy. Murine α-tubulin and γ-tubulin monoclonal antibodies were from Sigma, the antigen affinity-purified rabbit antibody to tubulin was kindly provided by M. Osborn. DNA was visualized by Hoechst 33342 dye. Separate samples were processed for immunoblotting with rabbit astrin antibody and peroxidase-conjugated swine anti-rabbit immunoglobulins (Dako, Denmark) using the ECL technique (Amersham Pharmacia Biotech). To confirm equal loading of gels used for astrin and control siRNAs, the blots were stripped (Re-Blot Western Blot Recycling Kit, Chemicon) and reprobed with the monoclonal vimentin V9 antibody (Osborn et al., 1984).

TUNEL test

For detection of apoptosis, a TUNEL test (In Situ Cell Death Detection Kit, Roche) was performed. Transfected cells grown for 60 hours were fixed in –20°C methanol for 6 minutes and treated with PBS containing 0.1% Triton X100 and 0.1% sodium citrate on ice for 2 minutes. Free 3′ ends of fragmented DNA were enzymatically labeled with FITC-tagged deoxynucleotide triphosphates using deoxynucleotidyl transferase (TdT). Labeled DNA fragments were monitored by fluorescence microscopy.

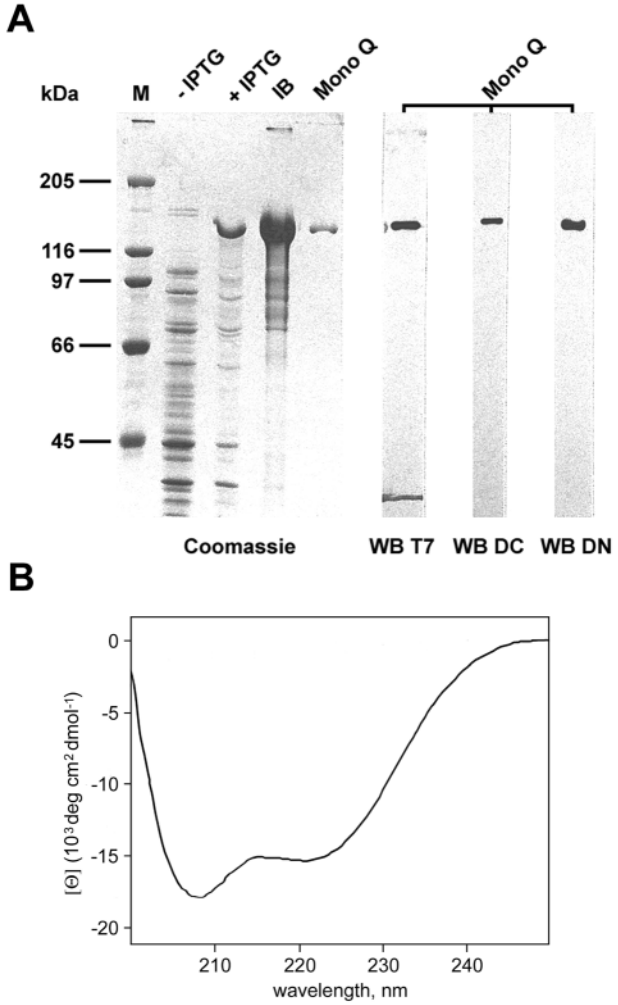

Fig. 2. (A) Purification of recombinant astrin. A Coomassie-stained gel showing bacterial extracts before (–IPTG) and 4 hours post-induction (+IPTG). The protein aggregated into inclusion bodies (IB) and was purified under denaturating conditions by anion exchange chromatography (Mono Q). Western blot (WB) analysis using a monoclonal T7-antibody against the tag-sequence and the two astrin antibodies (DC and DN) confirmed the identity of purified astrin. (B) CD spectroscopy of purified astrin in phosphate buffer containing 0.5 mM DTT.

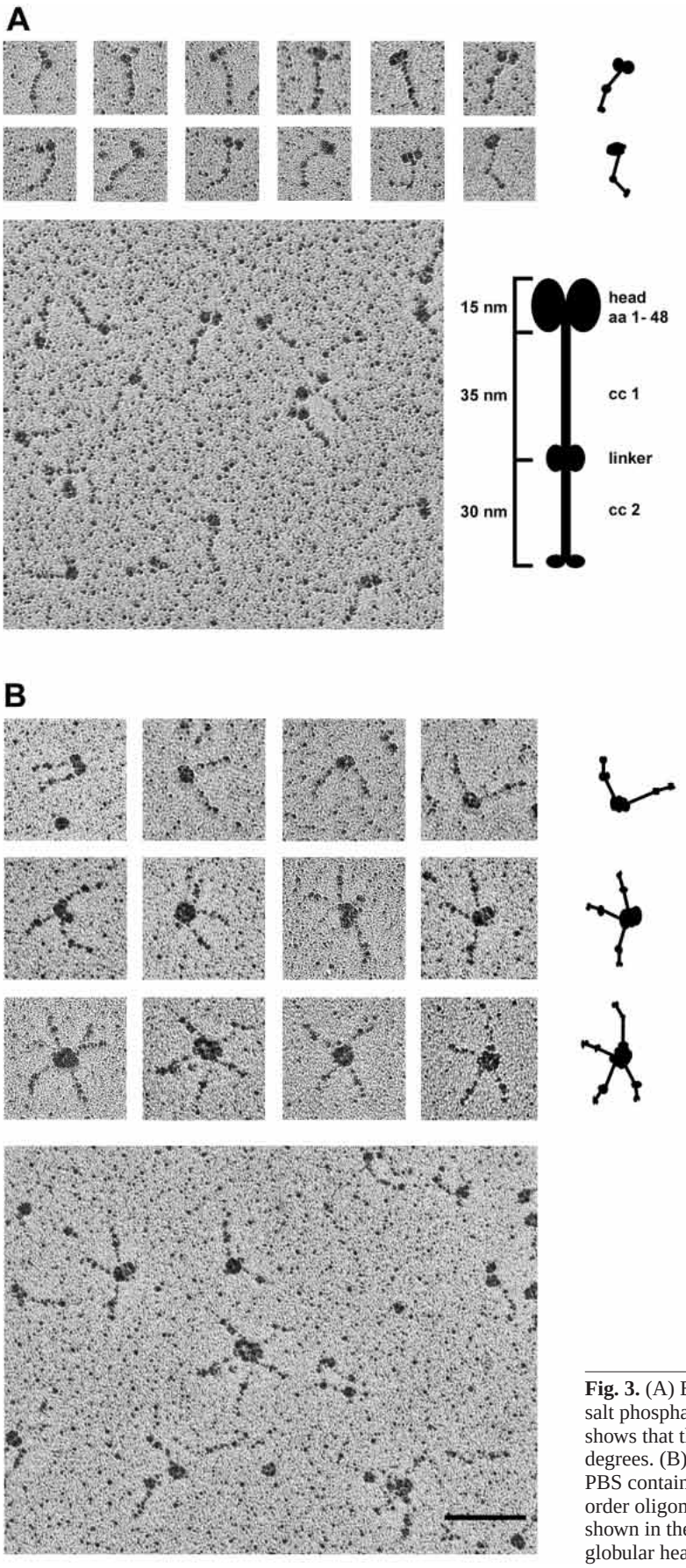

Results and Discussion

Astrin is a spindle-associated protein expressed in many human tissues and cell lines (Chang et al., 2001; Mack and Compton, 2001). In interphase cells it revealed a punctate cytoplasmic staining pattern that seemed to be independent of microtubules, but during mitosis it associated with the mitotic spindle in a microtubule-dependent manner (data not shown) (Chang et al., 2001; Mack and Compton, 2001).

Structure and domain organization of astrin

As previously noted (Mack and Compton, 2001), the astrin sequence shows similarities to a partial mouse clone of unknown function (Nehls et al., 1995) and to the rat Spag5 protein (Shao et al., 2001), which interacts with an outer dense filament (odf) protein (odf1) from sperm flagella (Shao et al., 2001). However, depletion of Spag5 revealed no phenotype, and Spag5-null mice were viable and fertile, suggesting that if Spag5 plays a role in spermatogenesis it is probably compensated for by other unknown proteins (Xue et al., 2002).

According to secondary structure predictions, the astrin sequence can be separated into several distinct domains (Fig. 1A). The N-terminal head domain (aa 1-481) of astrin is rich in proline (7.5%) together with serine and threonine residues, suggesting that astrin's function is regulated by phosphorylation in vivo. This hypothesis is supported by the finding of Chang, who showed that astrin is a substrate of cdk1 in vitro (Chang, 2001). In addition, four PXXP motifs in the astrin head domain may represent putative SH3-interaction sites, suggesting that astrin could be a target for regulatory proteins (Alexandropoulos et al., 1995; Yu et al., 1994). Three regions (amino acids 95 to 119, 287 to 330 and 463 to 477) are especially rich in Pro, Glu/Asp and Ser/Thr residues, respectively. These so-called PEST sequences are frequently found in proteins underlying rapid degradation through ubiquitin-protein ligase complexes. This degradation is regulated through phosphorylation of the PEST sequence motifs (Rechsteiner and Rogers, 1996; Rogers et al., 1986). Rapid protein degradation is an important regulatory mechanism in cell cycle regulation. Cyclins contain PEST sequences of the cyclin destruction box type, and phosphorylation of these motifs leads to ubiquitylation and degradation, which is a prerequisite for cell cycle progression (Rechsteiner and Rogers, 1996; Rogers et al., 1986). Amino acids 482 to 903 of astrin are predicted to be essentially α-helical except for a short interruption.

Fig. 3. (A) Electron microscope analysis of recombinant astrin-T7 in low salt phosphate buffer containing 2.5 mM DTT. The gallery of dimers shows that the flexible linker in the rod domain can be bent to varying degrees. (B) Electron microscope analysis of recombinant astrin-T7 in PBS containing 2.5 mM DTT. The overview shows formation of higher order oligomers. Examples of oligomers containing two to five dimers are shown in the gallery. Oligomerization is exclusively mediated by the globular head domains. Bar, 100 nm.

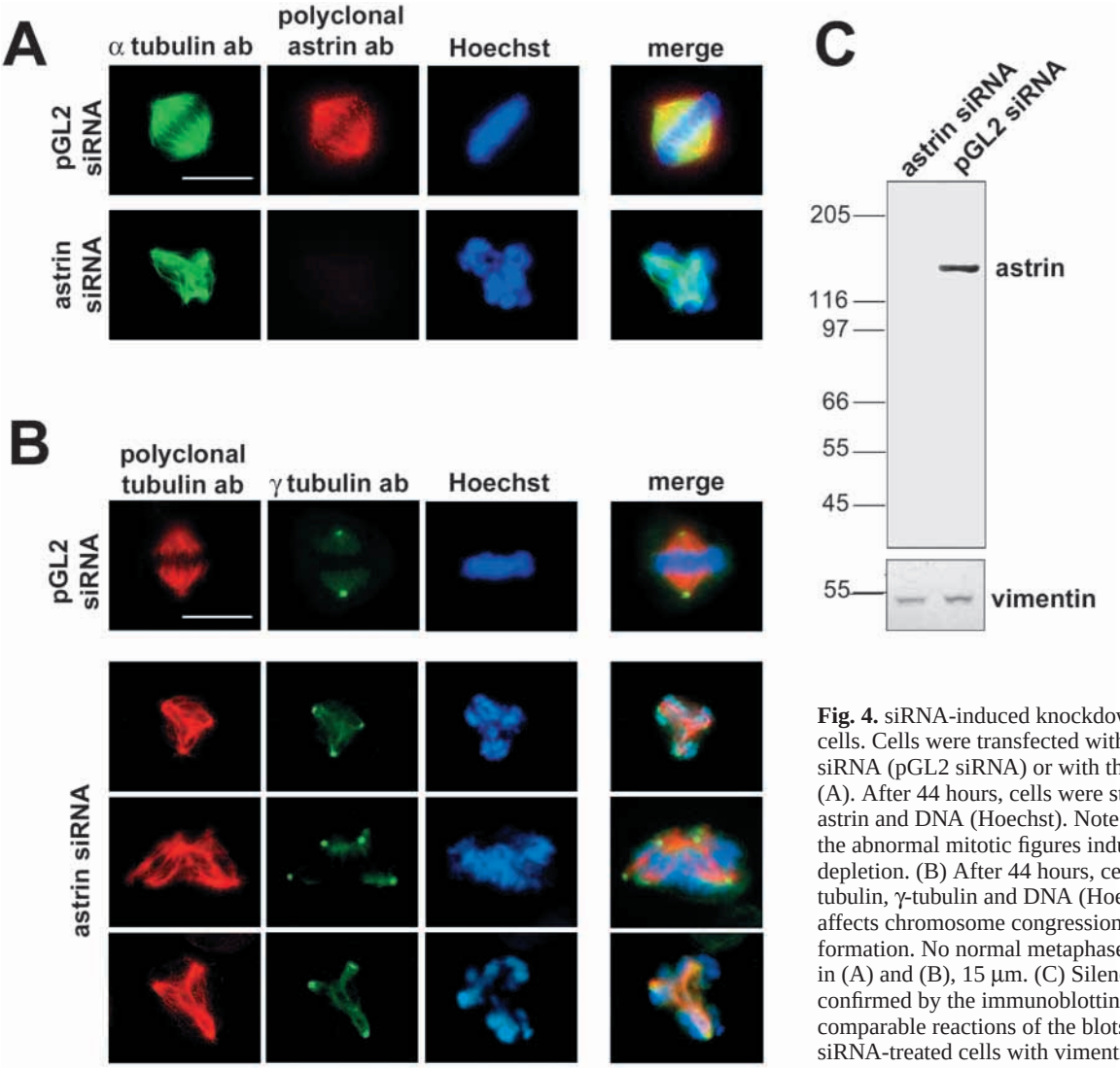

Fig. 4. siRNA-induced knockdown of astrin in HeLa cells. Cells were transfected with the luciferase control siRNA (pGL2 siRNA) or with the astrin-specific siRNA (A). After 44 hours, cells were stained for α-tubulin, astrin and DNA (Hoechst). Note the loss of astrin from the abnormal mitotic figures induced after astrin depletion. (B) After 44 hours, cells were stained for tubulin, γ-tubulin and DNA (Hoechst). Astrin depletion affects chromosome congression and proper spindle formation. No normal metaphase cells were found. Bars in (A) and (B), 15 μm. (C) Silencing of astrin was confirmed by the immunoblotting. The lower parts show comparable reactions of the blots of control and astrin-siRNA-treated cells with vimentin antibody.

Most of this region shows the heptad repeat pattern of coiled-coil proteins, suggesting dimerization and formation of a rod-like structure. Amino acids 904 to 965 are predicted to be non-α-helical owing to a high proline content (linker L). This linker region joins the first coiled-coil domain to a second coiled-coil region (amino acids 966 to 1175).

In order to analyze structure, domain organization and oligomerization of astrin, we used the purified recombinant protein. Astrin-T7 aggregated into inclusion bodies in *E. coli* and was purified under denaturing conditions by anion exchange chromatography. Fig. 2A shows a summary of the purification. Purified astrin-T7 was dialyzed against phosphate buffer (pH 7.5, containing 0.5 mM DTT), and CD spectroscopy was used to compare the actual and predicted α-helix content to ensure renaturation (Fig. 2B). The α-helix content was determined to be 55%, which is in good agreement with the predicted content (60%, compare Fig. 1A). Hence, we conclude that recombinant astrin refolded into its native structure.

Electron microscopy of astrin molecules in phosphate buffer revealed a 'lolly pop'-shaped structure with a prominent globular head and a rod domain with a flexible hinge (Fig. 3A). The length of the dimer in its extended version was approximately 80 nm. On the basis of structural predictions and electron microscopy, we propose a model according to which astrin forms parallel dimers via its α-helical coiled-coil domains. The N-terminal region forms a globular head domain, giving the dimers a lollipop-like structure. The first α-helical region with a heptad repeat pattern (aa 481 to 903) is predicted to form a rod domain of about 35 nm, which is in agreement with measurements from electron microscope images. The flexible linker corresponds to the L-domain, which contains the DEEPEST motif. Kinks of varying angular degrees indicate that this region represents a flexible joint in the stiff rod domain. The linker is followed by a second rod domain of 30 nm, representing the α-helical region from aa 966-1123 (Fig. 1A, Fig. 3A). Since the globular heads are on one side of the rods, the double-stranded coiled coils are parallel. Although the overall structure of astrin dimers resembles that of motor proteins, sequence analysis did not reveal any homology to motor domains, which have a well characterized and conserved protein module (Mack and

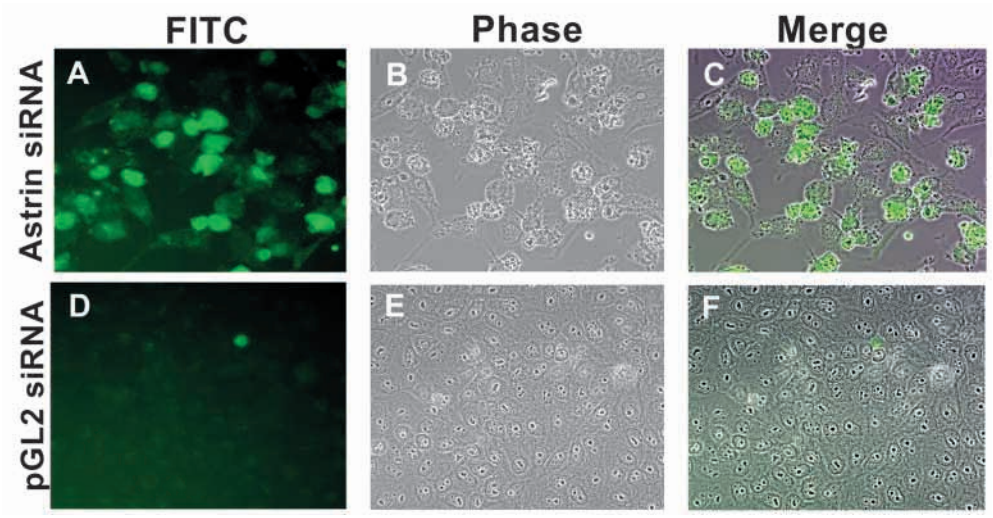

Fig. 5. Astrin silencing induces apoptosis. The TUNEL assay shows that many of the cells transfected with the astrin siRNA undergo apoptosis (green colour) 60 hours post-transfection (A-C). Cells transfected with the luciferase siRNA (pGL2) continue to grow (D-F). A single apoptotic cell was detected in this field. The phase image and the fluorescent image arising from the incorporation of FITC-labeled deoxynucleotides are superimposed (for details see Materials and Methods).

Compton, 2001; Bloom and Endow, 1995; Hirokawa et al., 1998b; Hirose and Amos, 1999; Kim and Endow, 2000; Kirchner et al., 1999; Miki et al., 2001; Moore and Endow, 1996).

In PBS (containing 2.5 mM DTT), the astrin dimers associated into higher order structures (Fig. 3B). Besides the dimers seen in low salt buffer, oligomers of two to five dimers were formed under physiological salt conditions. Oligomerization was exclusively mediated by the head domains, and higher oligomers resembled astral structures. These oligomers may have the potential to bundle microtubules and to crosslink other astrin-binding partners. Thus, astrin may provide a scaffold for crosslinking regulatory and structural components at the mitotic spindle.

Astrin is an essential protein of the spindle

Immunofluorescence analysis of endogenous and GFP-tagged astrin in HeLa cells confirmed the results of Mack and Compton and Chang et al. (Chang et al., 2001; Mack and Compton, 2001) and showed a punctate staining in the cytoplasm of interphase cells and colocalization with the spindle apparatus in mitotic cells (data not shown). For RNA interference mediated by duplexes of 21-nt RNAs on HeLa cells, the published protocol was used (Elbashir et al., 2001; Harborth et al., 2001). The siRNA sequence for targeting human astrin was from position 2639 to 2661 relative to the first nucleotide of the start codon. Control experiments used a siRNA sequence for firefly luciferase (pGL2). Phase microscopy showed that with time the astrin-siRNA-treated cells became growth arrested and that an increasing number of cells rounded up. Forty-four hours after transfection, more than 50% of the cells had rounded up. Indirect immunofluorescence microscopy was performed at this time using double staining with affinity-purified rabbit antibodies to astrin and a murine monoclonal α-tubulin antibody (Fig. 4A). Astrin silencing resulted in a strong decrease in astrin staining. Microtubule distribution and morphology were not affected in astrin-silenced interphase cells. However, mitotic cells showed a remarkable phenotype, with aberrant mitotic arrest and multipolar and highly disordered spindles indicating that astrin function is essential for progression through the cell cycle. Chromosomes did not congress to the spindle equator and remained dispersed (Fig. 4A,B). Staining of astrin-silenced cells with γ-tubulin antibody to visualize centrosomes clearly indicated fragmentation of centrosomes. γ-tubulin was present in all poles of the aberrant multipolar spindles after astrin depletion (Fig. 4B). Astrin silencing was also confirmed by immunoblotting experiments. Although cells transfected with the luciferase siRNA revealed a strong astrin band at 140 kDa, the silenced cells lacked a recognizable signal (Fig. 4C). The phenotype seen with astrin siRNA was somewhat similar to that seen after RNAi of the kinetochore-associated protein CENP-E (Harborth et al., 2001). Ablation of this protein by antisense RNA revealed flattened spindles and fragmentation of spindle poles, indicating that CENP-E contributes to the geometry and stability of bipolar spindles (Yao et al., 2000). Moreover, suppression of CENP-E leads to chronic activation of the mitotic checkpoint machinery, suggesting that CENP-E contributes to checkpoint silencing (Abrieu et al., 2000; Yao et al., 2000). In the astrin siRNA-treated cultures, the majority of the cells became apoptotic. A TUNEL assay performed at 60 hours post-transfection with astrin siRNA showed that 70% of the cells had entered apoptosis whereas control cells transfected with luciferase siRNA had hardly any apoptotic cells (Fig. 5).

The combined results show that astrin is an essential protein involved in early events of spindle formation at a stage prior to metaphase. Although it is currently not known how astrin contributes exactly to spindle organization, structural data suggest that astrin oligomers may function in microtubule bundling and/or providing a scaffold for crosslinking regulatory proteins to spindle microtubules. Since astrin is expressed not only throughout mitosis but also during interphase, and mRNA expression seems not to correlate with the proliferative activity of a tissue (e.g. relatively high expression in heart, data not shown), we assume that astrin has an additional function in interphase cells that remains to be determined.

We thank Jürgen Schünemann for expert technical assistance and Mary Osborn for interesting and critical discussions. This work was in part supported by grants of the DFG and the BMBF to M.H.

References

Abrieu, A., Kahana, J. A., Wood, K. W. and Cleveland, D. W. (2000). CENP-E as an essential component of the mitotic checkpoint in vitro. *Cell* **102**, 817-826.

Alexandropoulos, K., Cheng, G. and Baltimore, D. (1995). Proline-rich sequences that bind to Src homology 3 domains with individual specificities. *Proc. Natl. Acad. Sci. USA* **92**, 3110-3114.

Auffrey, C. and Rougeon, F. (1980). Purification of mouse immunoglobulin heavy-chain messenger RNAs from total myeloma tumor RNA. *Eur. J. Cell Biol.* **107**, 303-314.

Banks, J. D. and Heald, R. (2001). Chromosome movement: dynein-out at the kinetochore. *Curr. Biol.* **11**, R128-R131.

Bloom, G. S. and Endow, S. A. (1995). Motor proteins 1: kinesins. *Protein Profile* **2**, 1105-1171.

Chang, M. S., Huang, C. J., Chen, M. L., Chen, S. T., Fan, C. C., Chu, J. M., Lin, W. C. and Yang, Y. C. (2001). Cloning and characterization of hMAP126, a new member of mitotic spindle-associated proteins. *Biochem. Biophys. Res. Commun.* **287**, 116-121.

Compton, D. A. (2000). Spindle assembly in animal cells. *Annu. Rev. Biochem.* **69**, 95-114.

Elbashir, S. M., Harborth, J., Lendeckel, W., Yalcin, A., Weber, K. and Tuschl, T. (2001). Duplexes of 21-nucleotide RNAs mediate RNA interference in cultured mammalian cells. *Nature* **411**, 494-498.

Harborth, J., Elbashir, S. M., Bechert, K., Tuschl, T. and Weber, K. (2001). Identification of essential genes in cultured mammalian cells using small interfering RNAs. *J. Cell Sci.* **114**, 4557-4565.

Hatzfeld, M. and Weber, K. (1990). The coiled coil of *in vitro* assembled keratin filaments is a heterodimer of type I and II keratins; use of site-specific mutagenesis and recombinant protein expression. *J. Cell Biol.* **110**, 1199-1210.

Heald, R., Tournebize, R., Blank, T., Sandaltzopoulos, R., Becker, P., Hyman, A. and Karsenti, E. (1996). Self-organization of microtubules into bipolar spindles around artificial chromosomes in *Xenopus* egg extracts. *Nature* **382**, 420-425.

Hirokawa, N., Noda, Y. and Okada, Y. (1998a). Kinesin and dynein superfamily proteins in organelle transport and cell division. *Curr. Opin. Cell Biol.* **10**, 60-73.

Hirokawa, N., Noda, Y. and Okada, Y. (1998b). Kinesin and dynein superfamily proteins in organelle transport and cell division. *Curr. Opin. Cell Biol.* **10**, 60-73.

Hirose, K. and Amos, L. A. (1999). Three-dimensional structure of motor molecules. *Cell Mol. Life Sci.* **56**, 184-199.

Howell, B. J., McEwen, B. F., Canman, J. C., Hoffman, D. B., Farrar, E. M., Rieder, C. L. and Salmon, E. D. (2001). Cytoplasmic dynein/dynactin drives kinetochore protein transport to the spindle poles and has a role in mitotic spindle checkpoint inactivation. *J. Cell Biol.* **155**, 1159-1172.

Joshi, H. C. (1998). Microtubule dynamics in living cells. *Curr. Opin. Cell Biol.* **10**, 35-44.

Karsenti, E. and Vernos, I. (2001). The mitotic spindle: a self-made machine. *Science* **294**, 543-547.

Kim, A. J. and Endow, S. A. (2000). A kinesin family tree. *J. Cell Sci.* **113**, 3681-3682.

Kirchner, J., Woehlke, G. and Schliwa, M. (1999). Universal and unique features of kinesin motors: insights from a comparison of fungal and animal conventional kinesins. *Biol. Chem.* **380**, 915-921.

Lombillo, V. A., Nislow, C., Yen, T. J., Gelfand, V. I. and McIntosh, J. R. (1995). Antibodies to the kinesin motor domain and CENP-E inhibit microtubule depolymerization-dependent movement of chromosomes *in vitro*. *J. Cell Biol.* **128**, 107-115.

Mack, G. J. and Compton, D. A. (2001). Analysis of mitotic microtubule-associated proteins using mass spectrometry identifies astrin, a spindle-associated protein. *Proc. Natl. Acad. Sci. USA* **98**, 14434-14439.

Maney, T., Ginkel, L. M., Hunter, A. W. and Wordeman, L. (2000). The kinetochore of higher eucaryotes: a molecular view. *Int. Rev. Cytol.* **194**, 67-131.

Miki, H., Setou, M., Kaneshiro, K. and Hirokawa, N. (2001). All kinesin superfamily protein, KIF, genes in mouse and human. *Proc. Natl. Acad. Sci. USA* **98**, 7004-7011.

Moore, J. D. and Endow, S. A. (1996). Kinesin proteins: a phylum of motors for microtubule-based motility. *Bioessays* **18**, 207-219.

Nedelec, F. J., Surrey, T., Maggs, A. C. and Leibler, S. (1997). Self-organization of microtubules and motors. *Nature* **389**, 305-308.

Nehls, M., Luno, K., Schorpp, M., Pfeifer, D., Krause, S., Matysiak-Scholze, U., Dierbach, H. and Boehm, T. (1995). YAC/P1 contigs defining the location of 56 microsatellite markers and several genes across 3.4cM interval on mouse chromosome 11. *Mamm. Genome* **6**, 321-331.

Nicklas, R. B., Ward, S. C. and Gorbsky, G. J. (1995). Kinetochore chemistry is sensitive to tension and may link mitotic forces to a cell cycle checkpoint. *J. Cell Biol.* **130**, 929-939.

Osborn, M., Debus, E. and Weber, K. (1984). Monoclonal antibodies specific for vimentin. *Eur. J. Cell Biol.* **34**, 137-143.

Rechsteiner, M. and Rogers, S. W. (1996). PEST sequences and regulation by proteolysis. *Trends Biochem. Sci.* **21**, 267-271.

Rieder, C. L., Cole, R. W., Khodjakov, A. and Sluder, G. (1995). The checkpoint delaying anaphase in response to chormosome monoorientation is mediated by an inhibitory signal produced by unattached kinetochores. *J. Cell Biol.* **130**, 941-948.

Rieder, C. L. and Salmon, E. D. (1998). The vertebrate cell kinetochore and its roles during mitosis. *Trends Cell Biol.* **8**, 310-318.

Rogers, S., Wells, R. and Rechsteiner, M. (1986). Amino acid sequences common to rapidly degraded proteins: the PEST hypothesis. *Science* **234**, 364-368.

Saxton, W. M., Stemple, D. L., Leslie, R. J., Salmon, E. D., Zavortink, M. and McIntosh, J. R. (1984). Tubulin dynamics in cultured mammalian cells. *J. Cell Biol.* **99**, 2175-2186.

Shao, X., Xue, J. and van der Hoorn, F. A. (2001). Testicular protein Spag5 has similarity to mitotic spindle protein Deepest and binds outer dense fiber protein Odf1. *Mol. Reprod. Dev.* **59**, 410-416.

Tournebize, R., Popov, A., Kinoshita, K., Ashford, A. J., Rybina, S., Pozniakovsky, A., Mayer, T. U., Walczak, C. E., Karsenti, E. and Hyman, A. A. (2000). Control of microtubule dynamics by the antagonistic activities of XMAP215 and XKCM1 in *Xenopus* egg extracts. *Nat. Cell Biol.* **2**, 13-19.

Vasquez, R. J., Gard, D. L. and Cassimeris, L. (1999). Phosphorylation by CDK1 regulates XMAP215 function in vitro. *Cell Motil. Cytoskeleton* **43**, 310-321.

Walczak, C. E., Vernos, I., Mitchison, T. J., Karsenti, E. and Heald, R. (1998). A model for the proposed roles of different microtubule-based motor proteins in establishing spindle bipolarity. *Curr. Biol.* **8**, 903-913.

Wittmann, T., Hyman, A. and Desai, A. (2001). The spindle: a dynamic assembly of microtubules and motors. *Nat. Cell Biol.* **3**, E28-E34.

Xue, J., Tarnasky, H. A., Rancourt, D. E. and van Der Hoorn, F. A. (2002). Targeted disruption of the testicular SPAG5/deepest protein does not affect spermatogenesis or fertility. *Mol. Cell Biol.* **22**, 1993-1997.

Yao, X., Abrieu, A., Zheng, Y., Sullivan, K. F. and Cleveland, D. W. (2000). CENP-E forms a link between attachment of spindle microtubules to kinetochores and the mitotic checkpoint. *Nat. Cell Biol.* **2**, 484-491.

Yen, T. J., Li, G., Schaar, B. T., Szilak, I. and Cleveland, D. W. (1992). CENP-E is a putative kinetochore motor that accumulates just before mitosis. *Nature* **359**, 536-539.

Yu, H., Chen, Y. K., Feng, S., Dalgarno, D. C., Salmon, E. D. and Bloom, K. (1994). Structural basis for the binding of proline-rich peptides to SH3 domains. *Cell* **76**, 933-945.